Dissection of Tomato Lycopene Biosynthesis through Virus-Induced Gene Silencing[1][C][W][OPEN]

Elio Fantini[2], Giulia Falcone[2], Sarah Frusciante, Leonardo Giliberto, and Giovanni Giuliano*

Italian National Agency for New Technologies, Energy, and Sustainable Development, Casaccia Research Center, 00123 Roma, Italy (E.F., G.F., S.F., G.G.); Genelab, 96010 Palazzolo Acreide (SR), Italy (E.F., L.G.); and University of Rome "La Sapienza," 00185 Roma, Italy (S.F.)

ORCID ID: 0000-0001-6481-7560 (E.F.).

Lycopene biosynthesis in tomato (*Solanum lycopersicum*) fruits has been proposed to proceed through a poly-cis pathway catalyzed by phytoene synthase (PSY), two desaturases (phytoene desaturase [PDS] and ζ-carotene desaturase [ZDS]), and two cis-trans isomerases (ζ-carotene isomerase [ZISO] and prolycopene isomerase [CrtISO]). The mechanism of action of these enzymes has been studied in *Escherichia coli*, but a systematic study of their in vivo function is lacking. We studied the function of nine candidate genes (*PSY1*, *PSY2*, *PSY3*, *PDS*, *ZDS*, *ZISO*, *CrtISO*, *CrtISO-Like1*, and *CrtISO-Like2*) using virus-induced gene silencing (VIGS) coupled to high-resolution liquid chromatography coupled with diode array detector and mass spectrometry, which allowed the identification and quantitation of 45 different carotenoid isomers, including linear xanthophylls. The data confirm the confinement of the VIGS signal to the silenced fruits and the similarity of the phenotypes of *PSY1*- and *CrtISO*-silenced fruits with those of the *yellow flesh* and *tangerine* mutants. Light was able to restore lycopene biosynthesis in *ZISO*-silenced fruits. Isomeric composition of fruits silenced at different metabolic steps suggested the existence of three functional units, comprising PSY1, PDS/ZISO, and ZDS/CrtISO, and responsible for the synthesis of 15-cis-phytoene, 9,9′-di-cis-ζ-carotene, and all-trans-lycopene, respectively. Silencing of a desaturase (*PDS* or *ZDS*) resulted in the induction of the isomerase in the same functional unit (*ZISO* or *CrtISO*, respectively). All-trans-ζ-carotene was detectable in nonsilenced fruits, greatly increased in *ZDS*-silenced ones, and disappeared in *CrtISO-Like1*-/*CrtISO-Like2*-silenced ones, suggesting the existence of a metabolic side branch, comprising this compound and initiated by the latter enzymes.

Tomato (*Solanum lycopersicum*) is a member of the family Solanaceae. The large mutant collections and high-resolution genetic maps, together with its ease of transformation and simple diploid genetics, make tomato the best genetic model in the asterid clade (representing approximately 25% of all vascular plants) and a model system for fleshy fruit development. Its homozygous genome has been completely sequenced, unveiling approximately 35,000 protein-coding genes, generated through two consecutive whole-genome triplications, that occurred approximately 130 and 60 million years ago (Sato et al., 2012). The closest genetically well-characterized plant, Arabidopsis (*Arabidopsis thaliana*), diverged from tomato approximately 120 million years ago (Moore et al., 2010), and the different histories of polyploidization and subsequent gene loss of the two plants have resulted in different numbers of paralogs encoding enzymes for the biosynthesis of carotenoids (Fig. 1B). Thus, the conclusions drawn from the study of Arabidopsis mutants often do not apply to tomato.

Tomato is by far the largest dietary source of lycopene, a red linear carotene that is of particular nutritional interest, since its consumption is associated with lowered risk of cancer and cardiovascular disease (Rao and Agarwal, 2000). In plant leaves, lycopene is a metabolic intermediate in the biosynthesis of xanthophylls and is usually undetectable. By contrast, it accumulates in the chromoplasts of several fruits, including tomato and watermelon (*Citrullus lanatus*; Lewinsohn et al., 2005). Biosynthesis of lycopene from geranylgeranyl pyrophosphate (GGPP) has been proposed to proceed through a poly-cis pathway catalyzed by phytoene synthase (PSY), phytoene desaturase (PDS), ζ-carotene isomerase (ZISO), ζ-carotene desaturase (ZDS), and prolycopene isomerase (CrtISO; Fig. 1A). The mechanism of action of these enzymes has been studied in *Escherichia coli* cells expressing appropriate intermediates, or in cell-free systems, providing detailed insights on their mechanism of action (Bartley et al., 1999; Isaacson et al., 2004; Chen et al.,

[1] This work was supported by the European Commission ("High Quality Solanaceous Crops for Consumers, Processors, and Producers by Exploration of Natural Biodiversity" and "The Development of Tools and Effective Strategies for the Optimisation of Useful Secondary Metabolite Production In Planta" Projects), by the Italian Ministry of Agriculture ("Improving the Health and Functional Properties of Agricultural Commodities for Human and/or Animal Consumption" Project), and by the Italian Ministry of Research ("Integrated Knowledge for the Sustainability and Innovation of Italian Agri-Food" Project).

[2] These authors contributed equally to the article.

*Address correspondence to giovanni.giuliano@enea.it.

The author responsible for distribution of materials integral to the findings presented in this article in accordance with the policy described in the Instructions for Authors (www.plantphysiol.org) is: Giovanni Giuliano (giovanni.giuliano@enea.it).

[C] Some figures in this article are displayed in color online but in black and white in the print edition.

[W] The online version of this article contains Web-only data.

[OPEN] Articles can be viewed online without a subscription.

www.plantphysiol.org/cgi/doi/10.1104/pp.113.224733

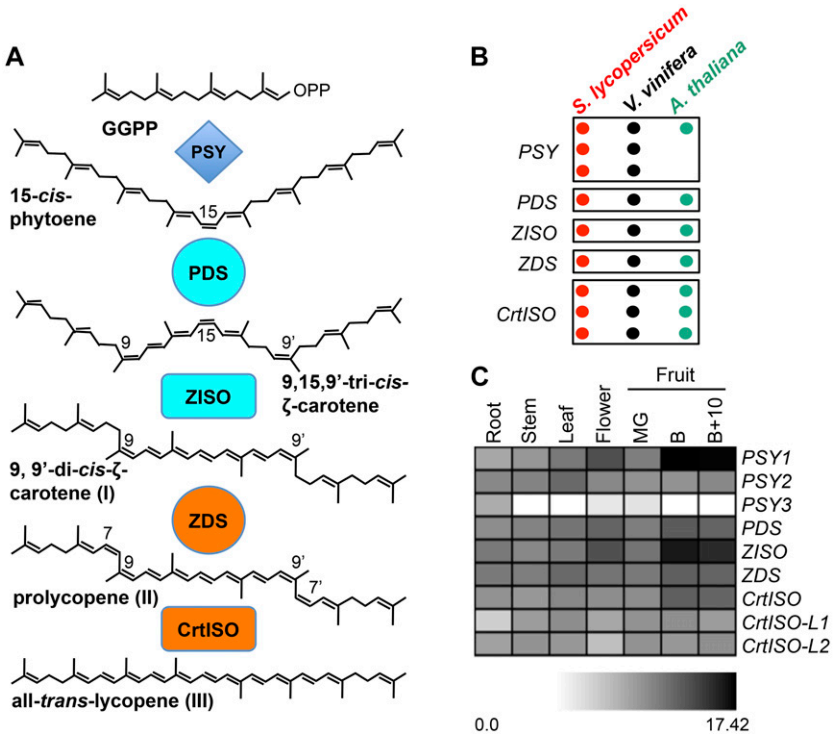

Figure 1. Lycopene biosynthesis pathway in tomato fruits. A, Proposed pathway, showing the main compounds and enzymes involved. B, Candidate genes involved in lycopene biosynthesis in tomato (red), Arabidopsis (green), and grape (black). Each dot represents one gene. C, Expression heat map (Log2 scale) of candidate lycopene biosynthesis genes in different tissues of tomato, analyzed by Illumina RNA-Seq. MG, Mature green fruit; B, breaker fruit; B+10, ripe fruit 10 d after breaker stage. Detailed data are shown in Supplemental Table S1. [See online article for color version of this figure.]

2010; Yu et al., 2011). However, knowledge on the transcriptional and posttranscriptional regulation and metabolic channeling in the pathway is still scarce and requires systematic in vivo studies using reverse genetic approaches. Such approaches have been possible, up to now, only in photosynthetic bacteria, where a large number of targeted gene knockouts can be produced in a matter of weeks (Giuliano et al., 1988).

Only two mutants are available in tomato, affecting lycopene biosynthesis from GGPP: *yellow flesh*, a loss-of-function mutant of the *PSY1* gene (Fray and Grierson, 1993), and *tangerine*, affecting the *CrtISO* gene (Isaacson et al., 2002). The *PDS* gene has been also studied using virus-induced gene silencing (VIGS; Orzaez et al., 2009; Romero et al., 2011). Additional mutants in the *PDS*, *ZDS*, and *ZISO* genes are available in Arabidopsis and maize (*Zea mays*; Hable et al., 1998; Li et al., 2007; Dong et al., 2007; Qin et al., 2007; Chen et al., 2010), two plants quite distant evolutionarily from tomato and with a very different type of fruit development.

VIGS is a high-throughput method for the study of gene function in plants (Baulcombe, 1999). The cloning of a gene fragment in the genome of an RNA virus, followed by the infection of the plant by the engineered virus, generates a double-stranded RNA molecule, which in turn triggers posttranscriptional silencing of the corresponding gene. Several viruses have been used for VIGS in tomato, including Potato Virus X (Giliberto et al., 2005) and Tobacco Rattle Virus (TRV; Liu et al., 2002). TRV is by far the most used virus, especially for silencing in fruit tissue (Fu et al., 2005; Orzaez et al., 2009). One of the main limitations of VIGS is its irregular distribution, preventing the exact quantification of the effects of gene silencing. This limitation has been alleviated through the use of a visual reporter system (Orzaez et al., 2009) based on the fruit-specific overexpression of the Delila (Del) and Rosea1 (Ros1) transcription factors, which cause anthocyanin accumulation (Fig. 2B). Silencing with TRV containing *Del* and *Ros1* sequences, together with those of the target gene(s), allows the dissection of silenced, anthocyanin-free fruit sectors from nonsilenced, anthocyanin-containing ones, thus facilitating the quantitative assessment of biochemical phenotypes (Fig. 2B).

The aim of this work is to dissect in vivo the biosynthesis of lycopene from GGPP in tomato fruits. Several novel candidate genes revealed by the tomato genome sequence were included in the study, for a total of nine genes: *PSY1*, *PSY2*, *PSY3*, *PDS*, *ZDS*, *ZISO*, *CrtISO*, *CrtISO-Like1* (*CrtISO-L1*), and *CrtISO-Like2* (*CrtISO-L2*; Fig. 1, B and C). Efficient silencing was obtained for most genes. The limited interference between the anthocyanin and lycopene biosynthesis pathways allowed the successful use of the visual reporter system for dissecting lycopene biosynthesis.

RESULTS

Construction and Assessment of the Silencing Vectors

Orzaez and coworkers generated transgenic tomato plants, named F6DR, overexpressing the Del and ROS1

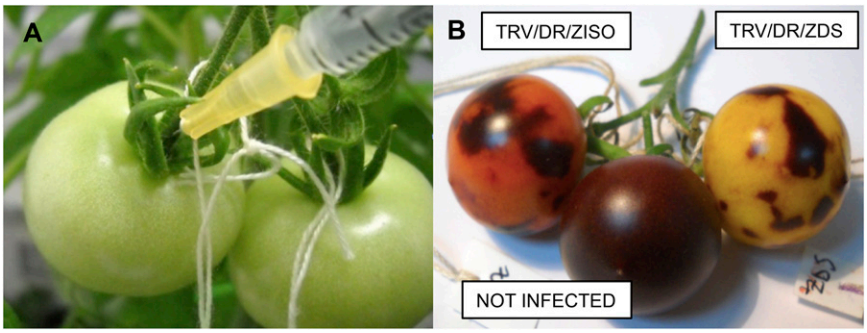

Figure 2. Fruit-specific VIGS of lycopene biosynthesis genes. A, Agroinjection of mature green F6DR fruits. B, Fruits from the same branch, injected with different constructs, display construct-specific phenotypes at ripening, confirming that the virus does not spread to adjacent fruits. [See online article for color version of this figure.]

transcription factors of *Antirrhinum majus* in a fruit-specific fashion. Ripe fruits of these plants have a deep purple pigmentation due to the accumulation of anthocyanins. Agroinjection of mature green fruits (Fig. 2A) with a TRV vector carrying fragments of the *Del* and *Ros1* genes (pTRV2/DR; Supplemental Fig. S1) resulted in the widespread silencing of anthocyanin biosynthesis (Fig. 2B). All enzymes in this study are encoded in tomato by single-copy genes, with the exception of *PSY*, which is encoded by three paralogs and *CrtISO*, which has two distant homologs, *CrtISO-L1* and *CrtISO-L2* (Sato et al., 2012; Fig. 1, B and C). The chromosomal positions of the different genes are shown in Supplemental Figure S2. All genes show some level of expression in fruits, with *PSY1* and *ZISO* being the most expressed and *PSY3* the least expressed (Fig. 1C; Supplemental Table S1).

We designed the silencing fragments in order to minimize off-target silencing. The percentage of identity of the silencing fragments was <50% with all tomato transcripts, including the other genes in the study, and the length of stretches with perfect identity to off-target transcripts was ≤19 nucleotides with all tomato transcripts and ≤14 with the other genes in the study, well below the 21-nucleotide threshold reported to cause off-target silencing (Xu et al., 2006; Supplemental Table S2). The sequences of the fragments are shown in Supplemental Figures S3 to S5. The fragments were cloned into pTRV2/DR (pTRV2/DR/GOI; Supplemental Fig. S1) and used for the silencing of F6DR fruits.

In order to verify the confinement of the VIGS signal, we infected different fruits on the same branch with the pTRV2/DR/ZDS and pTRV2/DR/ZISO vectors, which produce evidently different phenotypes. A noninfected fruit on the same branch served as a negative control. The results confirmed that the silencing signal does not spread outside the infected fruits (Fig. 2B), allowing the use of each fruit as single biological replicate (Orzaez et al., 2009). We then proceeded with the systematic silencing, using at least two different fruits from two different plants for each gene, for a total of at least four biological replicates. The anthocyanin-free fruit sectors were dissected and carotenoids were extracted using reverse-phase HPLC on a C30 column, coupled with online photodiode array (PDA) detection and high-resolution mass spectrometry (MS). The visual phenotypes of representative infected fruits and the resulting PDA chromatograms are shown in Figure 3. The analytical method used identified 45 different carotenoid compounds from tomato fruits, including several cis-isomers and hydroxylated compounds (Supplemental Table S3).

To assess whether anthocyanin accumulation per se, or its depletion in silenced sectors, had any effects on carotenoid biosynthesis, we measured the quantity of single carotenoid species in wild-type Moneymaker (MM) fruits, F6DR fruits, and anthocyanin-depleted sectors of F6DR fruits injected with TRV/DR (empty vector). The results (Figure 4) indicated an approximately 10% reduction of total carotenoid content between the wild-type line MM and F6DR and a further 2% reduction between F6DR and anthocyanin-depleted sectors. Infection with TRV/DR did not significantly affect the content of the pathway intermediates from phytoene to lycopene (Fig. 4; Supplemental Table S4). To assess the efficiency of silencing, we extracted RNA from anthocyanin-free fruit sectors and measured, via real-time reverse transcription (RT)-PCR, the transcript levels of the target gene. The levels were normalized to those of the *α-ACTIN* housekeeping transcript and then *Ros1* and *Del* levels were compared to those of uninfected F6DR fruits and carotenoid genes compared to those of TRV/DR fruits (Supplemental Fig. S6). Silencing of all genes was in the 85% to 100% range, with the exception of *PSY2* and *PSY3*, whose silencing was slightly above 70%. Within the range tested, there was not a major effect of the length of the silencing fragment on silencing efficiency. An inverse relationship was observed between the levels of expression of the endogenous gene and the severity of the silencing (Supplemental Fig. S6).

PSY1, PSY2, and PSY3

Three *PSY* genes are present in the tomato and grape (*Vitis vinifera*) genomes, in contrast with Arabidopsis that contains only one *PSY* (Fig. 1B; Supplemental Fig. S7). The tomato *PSY1-PSY2* pair was generated by a *Solanum*-specific whole-genome triplication (Sato et al., 2012). *PSY1* is one of the most highly expressed transcripts in ripe tomato fruits (Sato et al., 2012; Fig. 1C; Supplemental Table S1), and its function is impaired in the *yellow flesh* mutant, causing the lack of lycopene in fruits (Fray and Grierson, 1993). Silencing of *PSY1*

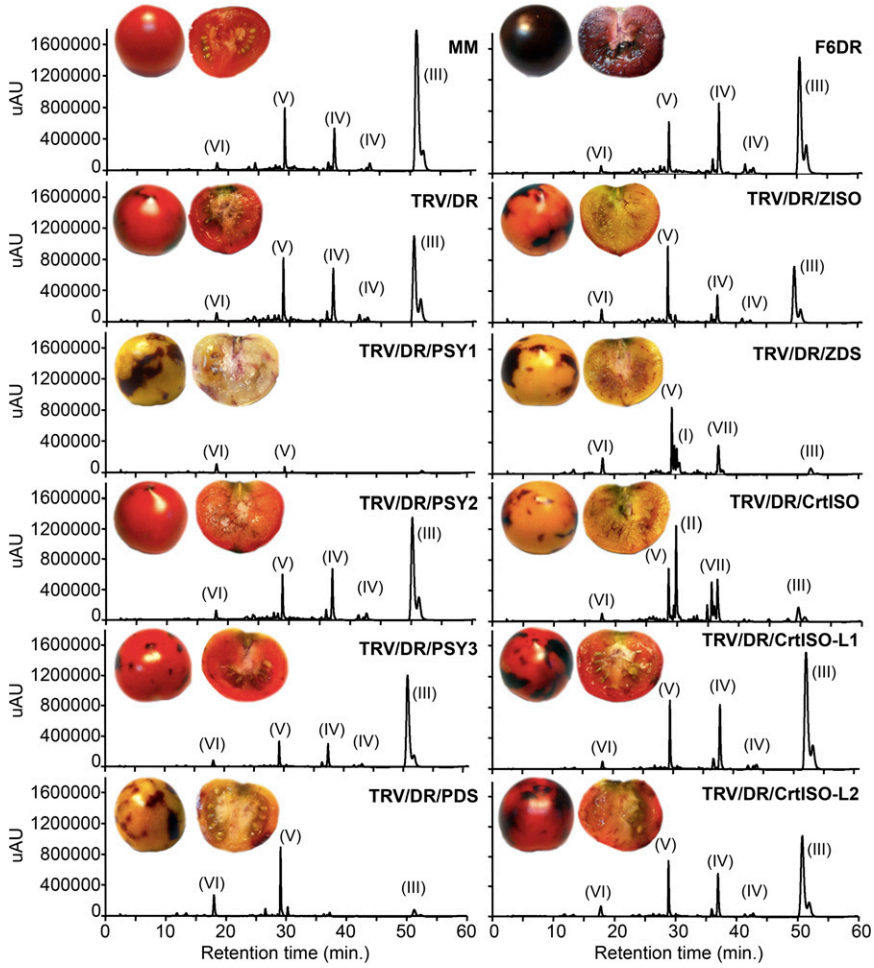

Figure 3. Visual and HPLC phenotypes of silenced fruits at B+10. The top two panels show wild-type MM fruits and F6DR transgenic fruits at B+10. The other panels show F6DR fruits injected with different silencing constructs. Representative visual phenotypes of the fruits and chromatographic profiles recorded at 450 nm are shown in each panel. Peak labeling is as follows: I to III indicate early compounds in Figure 1; IV, lycopene isomers; V, β-carotene; VI, lutein; and VII, neurosporene isomers. The online absorbance spectra of the different compounds are shown in Supplemental Figure S9. uAU, Micro-absorbance units. [See online article for color version of this figure.]

resulted in a phenotype highly similar to that of the *yellow flesh*^{3532} mutant, with complete disappearance of linear carotenoids and accumulation of trace amounts of lutein, β-carotene, and β-xanthophylls (Fig. 4; Supplemental Tables S5 and S6). Silencing of *PSY2* or *PSY3* was significantly less efficient than the other genes in the study (Supplemental Fig. S6) and did not result in an evident visual phenotype (Fig. 3). Silencing of *PSY3* resulted in small but significant reduction in early compounds (phytoene and phytofluene) as well as late ones (γ-carotene and δ-carotene; Supplemental Table S5).

PDS and ZDS

The pattern of expression of *PDS* and *ZDS* in tomato is similar, with *PDS* being slightly more expressed in flowers and *ZDS* in leaves and roots (Fig. 1C; Supplemental Table S1). Silencing of the two genes resulted in very similar visual phenotypes (Figure 3) but in quite different carotenoid compositions (Fig. 4; Supplemental Table S5). *PDS*-silenced fruits showed a 55% reduction of total carotenoids, with phytoene and phytofluene being the most abundant compounds, while *ZDS*-silenced fruits, besides the above-mentioned early intermediates, accumulated large amounts of ζ-carotene and traces of neurosporene, resulting in an increased carotenoid content with respect to TRV/DR fruits (Figure 4). Silencing of either gene resulted in almost complete disappearance of lycopene, while downstream compounds, such as β-carotene and lutein, were less affected. Overall, the biochemical phenotypes of the silenced fruits were in agreement with the function of the corresponding enzymes.

ZISO

Like *PDS* and *ZDS*, *ZISO* is a single-copy gene in tomato, grapevine, and Arabidopsis (Figure 1B), and it is highly expressed in tomato fruits (Fig. 1C; Supplemental Table S1). Its silencing resulted in a pale-red phenotype (Figure 3) due to a large reduction in lycopene and a compensatory increase of phytoene, phytofluene, and ζ-carotene (Fig. 4; Supplemental Table S5).

CrtISO, CrtISO-L1, and CrtISO-L2

Besides the canonical *CrtISO*, tomato, grapevine, and Arabidopsis contain two additional, distantly related

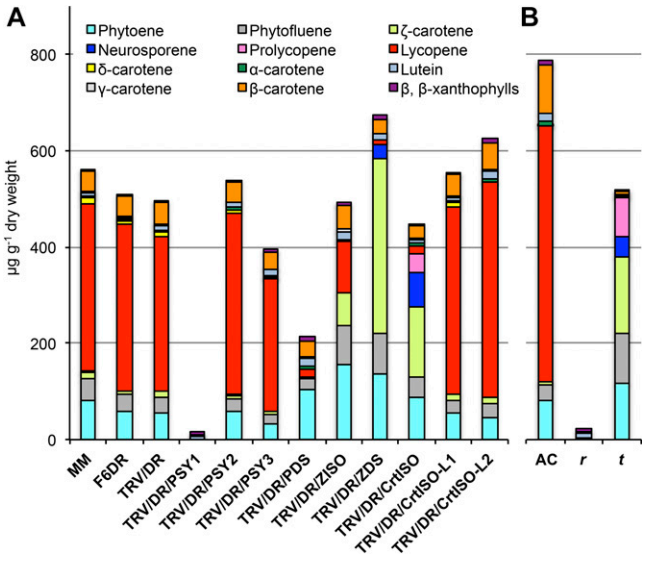

Figure 4. Carotenoid composition of silenced and mutant fruits at B+10. A, Amounts of the different carotenoid species in wild-type MM (LA2706), F6DR, and silenced fruits (Fig. 3), plotted as stacked bars. B, Amounts of the different carotenoid species for their wild-type Ailsa Craig (AC; LA2838A), *yellow flesh* (*r*; LA3532), and *tangerine* (*t*; LA3183) fruits, plotted as stacked bars. Detailed data are shown in Supplemental Tables S4 to S6. [See online article for color version of this figure.]

genes of unknown function, named *CrtISO-L1* and *CrtISO-L2* (Supplemental Fig. S8). Silencing of *CrtISO* caused the almost complete disappearance of lycopene and the accumulation of ζ-carotene, neurosporene, and prolycopene in a 4:2:1 ratio (Fig. 4; Supplemental Table S5). Fruits carrying the *tangerine*^{3183} allele of *CrtISO* presented a similar ratio (4:1:2; Fig. 4; Supplemental Table S6), different from the 1.6:1:1.7 ratio reported previously for the same allele in the M82 genetic background (Isaacson et al., 2002). Silencing of *CrtISO-L1* or *CrtISO-L2* did not cause an evident visible phenotype (Fig. 3). However, in *CrtISO-L2*-silenced fruits, lycopene was significantly increased (Fig. 4; Supplemental Table S5).

Light Partially Restores Lycopene Biosynthesis in *ZISO*-Silenced, But Not *CrtISO*-Silenced, Fruits

Leaves of *CrtISO* and *ZISO* mutants are initially pale and accumulate mainly cis-carotenoids, but upon exposure to light gradually increase all-trans carotenoid and chlorophyll content (Isaacson et al., 2002; Park et al., 2002; Chen et al., 2010). This phenomenon is not observed in nonphotosynthetic tissues, such as the endosperm of the maize *y9* mutant, or fruits of the tomato *tangerine* mutant, which accumulate cis-carotenoids even when exposed to light. We noticed that the residual red pigment accumulated by *ZISO*-silenced fruits was mainly concentrated in the superficial layers of the pericarp, suggesting that its accumulation may be enhanced by light penetrating from the outside of the fruit (Fig. 5B). To verify this hypothesis, we wrapped *ZISO*- and *CrtISO*-silenced fruits in aluminum foil immediately after agroinjection, while other agroinjected fruits on the same plant were left in normal light conditions (Fig. 5; Supplemental Table S7). Growth in the dark decreased fruit carotenoid content by approximately 40%, in agreement with previous observations that carotenoid biosynthesis in tomato fruits is stimulated by phytochrome and cryptochrome photoreceptors (Alba et al., 2000; Giliberto et al., 2005). However, in addition to increased carotenoid content, *ZISO*-silenced fruits grown in the light showed, with respect to their dark-grown counterparts, a significant increase of lycopene and reduction of cis-precursors, indicating that *ZISO* function can be partially substituted by light.

Isomers of Phytoene, Phytofluene, ζ-Carotene, Neurosporene, and Lycopene

The use of a C30 reverse-phase column coupled to online PDA detection and high-resolution MS allowed the separation and tentative identification of 45 different carotenoid species, including many cis-isomers and hydroxylated derivatives of phytoene, phytofluene, ζ-carotene, neurosporene, and lycopene. The retention time, absorption maxima, and accurate masses of these compounds are shown in Supplemental Table S3 and their online absorption spectra in Supplemental Figure S9. To verify the roles of the various genes in the desaturation/isomerization cascade, we quantified the main isomers (Fig. 6; Supplemental Table S8). The isomer composition of phytoene, ζ-carotene, and lycopene in *CrtISO*- and *ZISO*-silenced fruits grown in the light and in darkness was also analyzed (Supplemental Table S9).

PDS-silenced fruits accumulated, as expected, mainly 15-cis-phytoene, followed by 9,15-di-cis-phytofluene. In *ZISO*-silenced fruits, the main compound expected on the basis of the proposed pathway, i.e. 9,15,9′-tri-cis-ζ-carotene (Fig. 1), ranked 6th after 15-cis-phytoene, all-trans-lycopene, 9,15-di-cis-phytofluene, 9,9′-di-cis-ζ-carotene, and hydroxy phytoene (Fig. 6; Supplemental Table S8). Such low levels of 9,15,9′-tri-cis-ζ-carotene were not due to photoisomerization of the central 15-cis bond for two independent reasons: 15-cis-phytoene was a major compound both in the dark and in the light, and 9,15,9′-tri-cis-ζ-carotene did not increase in dark-grown fruits (Supplemental Table S9). In *ZDS*-silenced fruits, the main compound accumulated was the expected one, 9,15,9′-di-cis-ζ-carotene, followed by the earlier compounds 15-cis-phytoene, 9,15-di-cis-phytofluene, and 9,15,9′-tri-cis-ζ-carotene. Finally, in *CrtISO*-silenced fruits, the expected compound, prolycopene, ranked 3rd, after 9,9′-di-cis-ζ-carotene, 15-cis-phytoene, and 9,15-di-cis-phytofluene (Fig. 6; Supplemental Table S8). In other terms, silencing on an isomerase (*ZISO* and *CrtISO*, respectively) resulted in the accumulation of compounds diagnostic of an inhibition of the activity of the immediately upstream desaturase (*PDS* and *ZDS*,

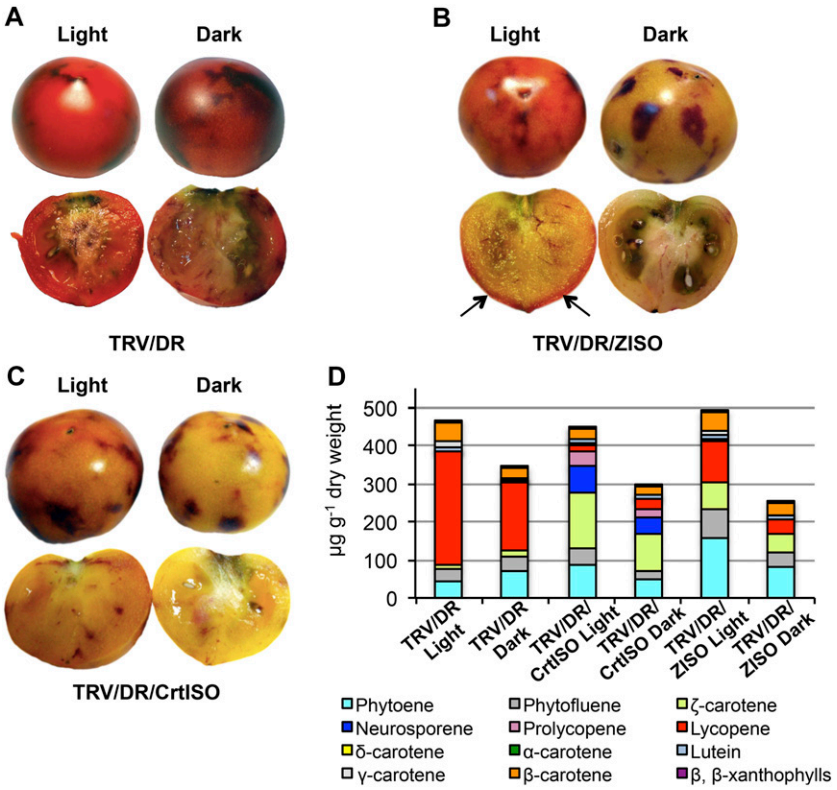

Figure 5. Light partially restores lycopene biosynthesis in *ZISO*-silenced, but not *CrtISO*-silenced, fruits. Agroinjected fruits were put in darkness (right) or left in the light (left) until B+10, and then anthocyanin-free sectors were dissected and analyzed by HPLC. A to C, Visual phenotypes. Arrows point at lycopene accumulation in peripheral tissues of light-grown, *ZISO*-silenced fruits. D, Carotenoid composition of samples. Data are the average of four biological replicates. Detailed data are shown in Supplemental Table S7. [See online article for color version of this figure.]

respectively). As discussed below, we consider this an indication of metabolic channeling.

All-trans-ζ-carotene is present, albeit at very low levels, in TRV/DR fruits (Fig. 6; Supplemental Table S8). This compound showed a significant increase in *ZDS*-silenced fruits, and it disappeared in *CrtISO-L1*- and *CrtISO-L2*-silenced ones (Fig. 6; Supplemental Table S8), indicating that these genes may have a role in its metabolism.

Transcriptional Regulation

We measured expression levels of the target gene, as well as of the off-target ones, by quantitative real-time RT-PCR. Several off-target regulatory effects were observed in silenced fruits (Fig. 7). First, a weak silencing of *PSY2* and *PSY1* (albeit at nonsignificant levels) was observed in *PSY3*-silenced fruits, suggesting that in spite of the careful design of the silencing fragment (Supplemental Table S2), some off-target silencing of the other two members of the family occurs. Second, the *PDS* transcript was silenced in *PSY1*-silenced fruits. This could be due to off-target silencing or to the existence of a regulatory loop, whereby the lack of phytoene in *PSY1*-silenced fruits (Fig. 4) represses the transcription of the *PDS* gene. Since we did not observe *PDS* repression in fruits of the *yellow flesh* mutant (Supplemental Fig. S10), which are also devoid of phytoene (Fig. 4), we favor the first hypothesis. Third, silencing of the desaturases (*PDS* and *ZDS*, respectively) was associated with a significant induction of the isomerases acting immediately downstream (*ZISO* and *CrtISO*, respectively). These inductions cannot be explained in terms of off-target silencing, and we therefore attribute them to bona fide regulatory loops acting in the fruit.

DISCUSSION

The biosynthesis of lycopene from GGPP is perhaps the most intensely studied biochemical pathway in tomato. In spite of this, until now, forward or reverse genetic data were available for only three genes: *PSY1* and *CrtISO*, based on the study of the *yellow flesh* and *tangerine* mutants (Clough and Pattenden, 1983; Fray and Grierson, 1993; Isaacson et al., 2002); and *PDS*, based on VIGS (Orzaez et al., 2009; Romero et al., 2011). With the exception of the study by Clough and Pattenden (1983), none of the other studies used high-resolution chromatographic methods, essential for the identification of the various isomeric intermediates.

The recent discoveries of *ZISO* in maize and Arabidopsis (Chen et al., 2010) and of the existence, in the tomato genome, of a third *PSY* paralog and of two *CrtISO*-like genes (Sato et al., 2012) increased the number of candidate genes to 9, of which six had not been genetically characterized in tomato and four (*PSY2*, *PSY3*, *CrtISO-L1*, and *CrtISO-L2*) in any plant species. We decided to study the function of all nine genes in the same genetic background and experimental conditions, combining a fruit-specific VIGS methodology (Orzaez et al., 2009) with C30 reverse-phase chromatography (Fraser et al., 2007),

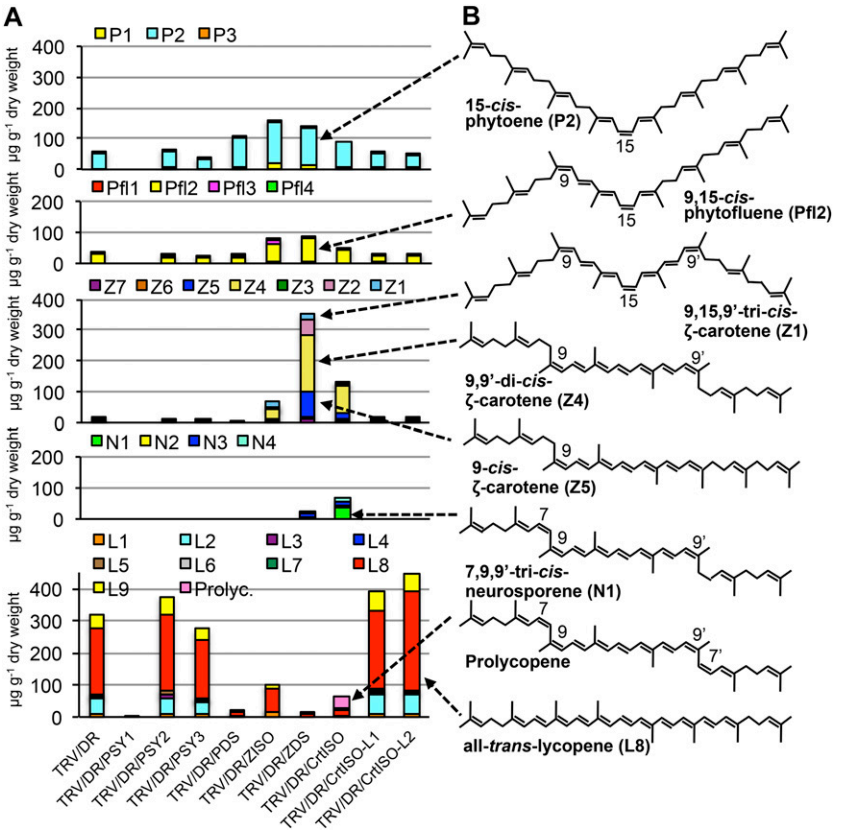

Figure 6. Isomer composition of silenced fruits. A, Levels of carotenoid isomers in silenced fruits. Detailed data are shown in Supplemental Table S8. B, Structure of the main isomers accumulated. P1, Hydroxy phytoene; P2, 15-cis-phytoene; P3, all-trans-phytoene; Pfl1, hydroxy phytofluene; Pfl2, 9,15-di-cis-phytofluene; Pfl3 and Pfl4, unidentified phytofluene isomers; Z1, 9,15,9′-tri-cis-ζ-carotene; Z2 and Z3, unidentified ζ-carotene isomers; Z4, 9,9′-di-cis-ζ-carotene; Z5, 9-cis-ζ-carotene; Z6, all-trans-ζ-carotene; Z7, hydroxy ζ-carotene; N1, 7,9,9′-tri-cis-neurosporene; N2 to N4, unidentified neurosporene isomers; L1, 13-cis-lycopene; L2, 5,13′-di-cis-lycopene; L3, 9-cis-lycopene; L4, 5,9′-cis-lycopene; L5, hydroxy lycopene; L6 and L7, unidentified lycopene isomers; L8, all-trans-lycopene; L9, 5-cis-lycopene; Prolyc, prolycopene (7,9,9′,7′-tetra-cis-lycopene). [See online article for color version of this figure.]

online photodiode array spectrophotometry, and high-resolution (Orbitrap) MS, allowing an unprecedented accuracy in the identification of the various compounds (Supplemental Table S3).

The VIGS visual reporter system developed by Orzaez et al. (2009) is based on the depletion of anthocyanins following the silencing of the *Del* and *Ros1* transgenes in the F6DR genetic background. As for any reporter system based on the accumulation of an endogenous metabolite, some level of interference with the metabolic pathway under study is expected. In the case of lycopene biosynthesis, this interference is very limited, as shown by the very similar levels of phytoene, phytofluene, ζ-carotene, and lycopene accumulated by F6DR fruits and their TRV/DR-silenced, anthocyanin-depleted sectors (Supplemental Table S4). The same metabolites show much higher variations in different genetic backgrounds, such as MM and AC (Supplemental Table S4), confirming the importance of using isogenic lines when performing biochemical genetic studies on the carotenoid pathway. Given the large number of different genetic backgrounds in which tomato mutants have been isolated, and the long time necessary to introgress a mutation from one genetic background to another, VIGS has, in our opinion, a clear edge over forward genetics for the rapid study of multigene pathways in the same genetic background. Of course, care should be taken, as was done in this case, to compare sectors silenced with TRV/DR/gene of interest with sectors silenced with TRV/DR alone. Our data confirm previous observations that the silencing signal remains confined to the agroinfiltrated fruit (Fu et al., 2005; Orzaez et al., 2009) rather than spreading systemically to the whole plant through the phloem, as is usually the case for silencing in leaves of the *Solanaceae* (Liang et al., 2011).

Linear Xanthophylls

The use of liquid chromatography (LC)-MS allowed the unambiguous identification of monohydroxylated derivatives of phytoene, phytofluene, ζ-carotene, neurosporene, and lycopene (Supplemental Table S3). The presence of hydroxy phytoene and hydroxy lycopene (lycoxanthin) had been reported previously in tomato fruits (Curl, 1961; Fray et al., 1995), albeit this identification did not involve MS. The exact structure of these compounds, as well as their enzymatic versus nonenzymatic origin, deserves further investigation. We observe that hydroxy phytoene and hydroxy ζ-carotene increase and hydroxy lycopene decreases in *PDS*- and *ZDS*-silenced fruits, suggesting that the former may be converted into the latter by PDS and ZDS. A desaturase accepting hydroxy neurosporene as a substrate has been described in purple photosynthetic bacteria, where it catalyzes the synthesis of linear xanthophylls spheroidene, demethylspheroidene, and spheroidenone (Giuliano et al., 1988).

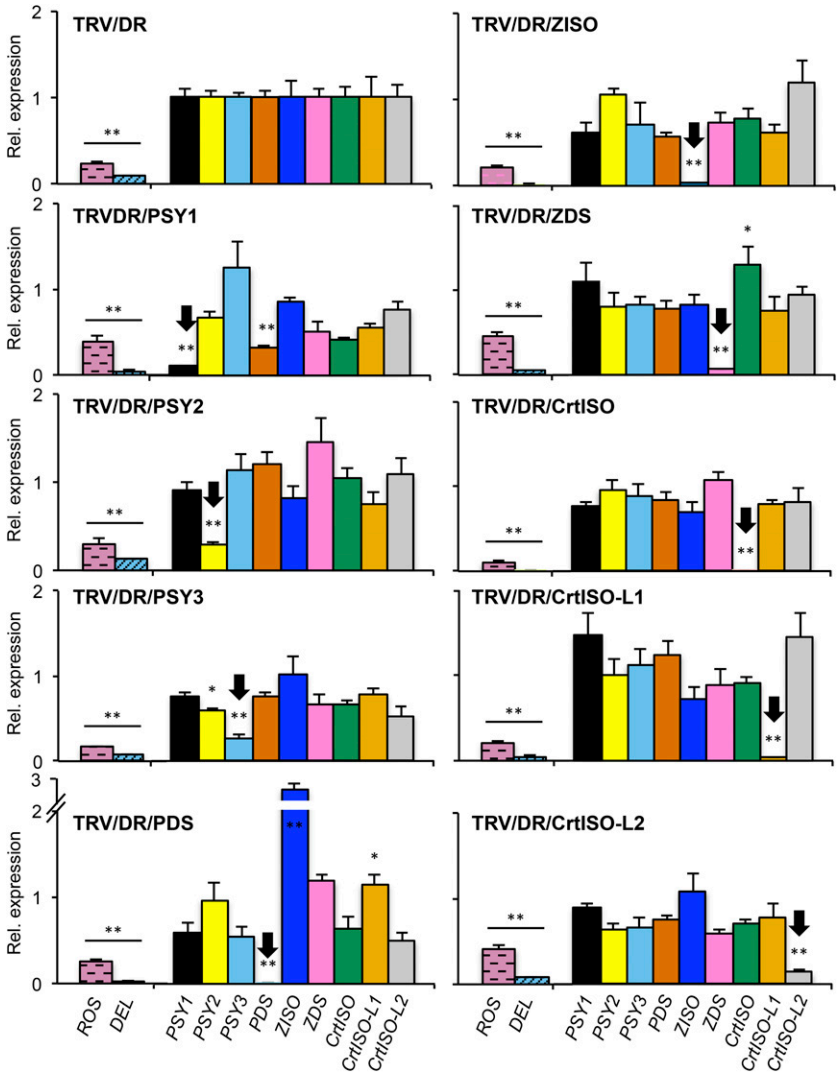

Figure 7. Gene expression in silenced tissues. Each panel shows gene expression in anthocyanin-free sectors of F6DR fruits injected with the construct indicated. Transcript levels of the *ROS* and *DEL* transgenes and of the different carotenoid genes shown in Figure 1 were measured through real-time RT-PCR and were first normalized for expression of the housekeeping α-*ACTIN* gene. The *ROS* and *DEL* transcript levels were normalized to those in uninfected fruits, while carotenoid transcript levels were normalized to those in TRV/DR fruits. Target genes (indicated by black arrows) show 70% to 99% silencing. Additionally, some nontarget genes show significant repression or induction (**P* value < 0.05; ***P* value < 0.01). Data are the average ± SD of at least three biological replicates. [See online article for color version of this figure.]

PSY

PSY (EC 2.5.1.32) catalyzes the head-to-head condensation of two molecules of GGPP to yield one molecule of 15-cis-phytoene, the first dedicated compound in the carotenoid pathway (Fig. 1A). Synteny analyses suggest that the *PSY1-PSY2* gene pair was generated by the *Solanum* whole-genome triplication that occurred approximately 60 million years ago (Sato et al., 2012), while *PSY3* is much more ancient and is possibly the ortholog of the *PSY3* gene found in cereals, which has been implicated in root abscisic acid biosynthesis (Li et al., 2008; Welsch et al., 2008). Silencing of *PSY1* resulted in a phenotype almost indistinguishable from that of the *yellow flesh* mutant, resulting in the complete disappearance of linear compounds and a decrease of cyclic carotenoids (α- and β-carotenes and xanthophylls; Fig. 3; Supplemental Table S5). *PSY2* silencing resulted in only a slight decrease of γ-carotene, while *PSY3* silencing caused the additional decrease of phytoene, phytofluene, ζ-carotene, and δ-carotene (Fig. 3; Supplemental Table S5). This is somewhat surprising because *PSY3* is expressed in fruits at very low levels and only at the MG stage (Fig. 1C; Supplemental Table S1). It must be noted, however, that *PSY2* and *PSY3* were silenced less efficiently (70%–75%) than the other genes in the study (85%–100%; Supplemental Fig. S6) and that the *PSY3* construct cross-silenced weakly the *PSY2* and *PSY1* genes (Fig. 7). We conclude that *PSY2* and *PSY3* do not play major roles in fruit lycopene biosynthesis, albeit a minor role cannot be excluded or confirmed on the basis of these data.

PDS and ZDS

PDS (EC 1.3.5.5) and ZDS (EC 1.3.5.6) catalyze the desaturation of 15-cis-phytoene and 9,9′-di-cis-ζ-carotene, respectively, through a poly-cis pathway (Bartley et al., 1999; Fig. 1A). They are encoded by single genes in tomato, grape, and Arabidopsis (Fig. 1B). Mutation of the two genes in the Arabidopsis *pds3* and *scd1* mutants

(Dong et al., 2007; Qin et al., 2007) results in impairment of xanthophyll and chlorophyll accumulation and in the accumulation of phytoene and ζ-carotene, respectively. Silencing of *PDS* in tomato fruits results in a 55% reduction of total carotenoids (Fig. 4), in contrast with the higher levels accumulated by leaves of the Arabidopsis *pds3* mutant or of *PDS*-silenced tobacco (*Nicotiana tabacum*; Busch et al., 2002; Qin et al., 2007). This suggests that different regulatory mechanisms may operate in chloroplast- versus chromoplast-containing tissues. *ZDS*-silenced tomato fruits accumulate mainly 9,9′-di-cis-ζ-carotene (Fig. 6), confirming that isomerization of the 15-cis double bond can occur before 7,7′ desaturation by ZDS, as proposed previously (Chen et al., 2010). In contrast with *PDS*-silenced fruits, *ZDS*-silenced ones accumulate higher levels of total carotenoids with respect to control fruits. This has several possible explanations: *PDS*-silenced fruits show an approximate 3-fold increase in *ZISO* expression, which might divert the carbon flux into a yet undescribed side branch, resulting in decreased accumulation of carotenoid intermediates; an alternative explanation is that the main compounds accumulated in *PDS*- and *ZDS*-silenced fruits (15-cis-phytoene and 9,9′-di-cis-ζ-carotene, respectively) show different stability.

ZISO and CrtISO

ZISO (EC 5.2.1.12) is encoded by a single gene in tomato, grape, and Arabidopsis (Fig. 1B), and it is highly expressed in tomato fruits (Fig. 1C). ZISO was first defined by the maize *y9* and Arabidopsis *zic1* mutants, which accumulate 9,15,9′-tri-cis-ζ-carotene in leaves (Li et al., 2007; Chen et al., 2010). When expressed in *E. coli* in combination with PDS, ZISO results in the isomerization of the 15-cis bond of phytoene (Chen et al., 2010), suggesting that it is either itself an isomerase or that it is required for the functioning of PDS as an isomerase. Both hypotheses are plausible, since both ZISO and PDS bear similarities to known carotenoid isomerases, i.e. D27 (Alder et al., 2012) and CrtISO (Isaacson et al., 2002), respectively. Our data support two aspects of the model proposed by Chen et al.: First, ZISO is required for the conversion of 15-cis-phytoene into downstream compounds bearing a trans double bond in this position; and second, in the absence of ZISO, light can partially compensate for its function. However, the exact mechanism through which this compensatory effect is exerted in tomato fruits deserves further investigation: *ZISO*-silenced fruits grown in the dark present, if anything, a lower ratio of tri-cis- to di-cis-ζ-carotene than their light-grown counterparts (Supplemental Table S9).

CrtISO (EC 5.2.1.13) was first defined by the Arabidopsis *ccr2* and the tomato *tangerine* mutants (Isaacson et al., 2002; Park et al., 2002). The main compounds accumulated by *ccr2* are 7,9,7′,9′-tetra-cis-lycopene (prolycopene) and a ζ-carotene isomer termed pro-ζ-carotene (Park et al., 2002), while the isomeric composition of ζ-carotene accumulated by *tangerine* was not defined (Isaacson et al., 2002). CrtISO exhibits homology to carotene desaturases (Giuliano et al., 2002), and, when expressed in *E. coli*, it is able to isomerize adjacent cis-double bonds at C7 and C9 pairwise into the trans-configuration (Isaacson et al., 2004). *ZISO*- and *CrtISO*-silenced tomato fruits accumulate 15-cis-phytoene and 9,9′-di-cis-ζ-carotene, respectively, as the main compounds (Fig. 6; Supplemental Table S8). This composition is highly different from that expected on the basis on the proposed mechanisms of action of the two enzymes and a possible indication of metabolic channeling (see below).

CrtISO-L1 and CrtISO-L2

These two genes are distantly related to *CrtISO* and are present in single copy in tomato, grape, and Arabidopsis. Comparison of the protein products suggests that they are orthologous to each other and that their divergence predates the asterid-rosid divergence (Supplemental Fig. S8). Both *CrtISO-L1* and *CrtISO-L2* silencing caused the disappearance of all-trans-ζ-carotene. This carotenoid has been identified previously in plant extracts (Park et al., 2002; Breitenbach and Sandmann, 2005), but, since it is not an intermediate in the plant poly-cis lycopene biosynthetic pathway, its enzymatic versus nonenzymatic origin is debated. Several lycopene isomers, including all-trans-lycopene, were increased in both *CrtISO-L1*- and *CrtISO-L2*-silenced fruits, but more significantly in the latter (Fig. 6; Supplemental Table S8). Based on these data, we speculate that CrtISO-L1 and/or CrtISO-L2 may initiate a competing branch with respect to the one leading to all-trans-lycopene that leads to hitherto undefined isoprenoids through all-trans-ζ-carotene. Further experimentation in *E. coli* is needed to verify this hypothesis.

Metabolic Channeling

According to the enzymatic mechanisms elucidated in *E. coli*, silencing of *PDS* is expected to cause the accumulation of all-trans-phytoene, silencing of *ZISO* the accumulation of 9,15,9′-tri-cis-ζ-carotene, silencing of *ZDS* the accumulation of 9,9′-di-cis-ζ-carotene, and silencing of *CrtISO* the accumulation of prolycopene. The real situation observed in vivo is quite different: Silencing of each enzymatic step results in the accumulation of a gradient of intermediates, peaking at different compounds: 15-cis-phytoene for PDS and ZISO, and 9,9′-di-cis-ζ-carotene for ZDS and CrtISO, (Fig. 6). Based on this, we propose the following model (Fig. 8): (1) In tomato fruits, the PSY1, PDS/ZISO, and ZDS/CrtISO enzymes form three functional catalytic units responsible for the synthesis of 15-cis-phytoene, 9,9′-di-cis-ζ-carotene, and all-trans-lycopene, respectively. (2) Repression of the isomerase function within each of the two latter units results in impaired function of the corresponding desaturase, leading to the accumulation of the earliest compound entering the unit (15-cis-phytoene and 9,9′-di-cis-ζ-carotene, respectively).

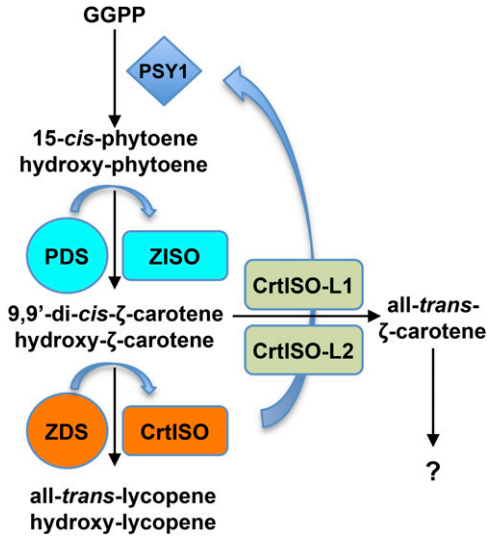

Figure 8. Proposed model for lycopene biosynthesis in tomato fruits. Three metabolic units, composed of PSY1, PDS/ZISO, and ZDS/CrtISO, catalyze the synthesis of 15-cis-phytoene, 9,9′-di-cis-ζ-carotene, and all-trans-lycopene (and of their hydroxylated derivatives). CrtISO-L1 and -L2 are active in a metabolic side branch comprising all-trans-ζ-carotene. Blue arrows indicate regulatory loops inducing specific transcripts in response to the inhibition of specific biosynthetic steps. [See online article for color version of this figure.]

The existence of functional catalytic units, or metabolons, grouping together several sequential enzymes of a metabolic process has long been hypothesized (Sweetlove and Fernie, 2013). These units present several theoretical advantages, such as improved kinetics due to the accelerated diffusion of the substrate from one enzyme to the next, improved access to common cofactors, and sequestration of toxic or labile intermediates. While some metabolic pathways do not appear to be limited by diffusion (Sweetlove and Fernie, 2013), this may hold true for the carotenoid metabolic pathway, where the substrates are bulky and insoluble in aqueous environments. Evidence for large complexes involving carotenoid biosynthesis enzymes has been provided by several authors (Candau et al., 1991; Bonk et al., 1997; Lopez et al., 2008; Quinlan et al., 2012).

Transcriptional Regulation

A large set of experimental data supports the existence, in the carotenoid pathway, of regulatory loops regulating the abundance of key transcripts in response to the operation of the pathway: In tomato leaves, the *PDS* promoter is up-regulated when carotenoid accumulation is inhibited (Giuliano et al., 1993; Corona et al., 1996). We did not find an indication of this regulatory loop in fruits, suggesting that it may be active only in photosynthetic tissues. A second, fruit-specific loop has been proposed recently to explain the epistatic behavior of *tangerine* over the *yellow flesh*^{2997} allele, which eliminates transcription of *PSY1* in fruits. When this allele is introduced in a homozygous *tangerine* background, *PSY1* transcription is restored, allowing the accumulation of prolycopene. Thus, the phenotype of the double *tangerine yellow flesh*^{2997} mutant is more similar to *tangerine* than to *yellow flesh* (Kachanovsky et al., 2012). The authors hypothesized that prolycopene, or a metabolite thereof, was the signal mediating *PSY1* induction. We didn't see any *PSY1* induction in *CrtISO*-silenced or mutant ripe fruits (Fig. 7; Supplemental Fig. S10). Since these fruits accumulated much lower prolycopene levels than those analyzed by Kachanovsky and coworkers, we hypothesize that, according to their model, a minimum level of prolycopene is required to attain *PSY1* transcript induction.

The *ZISO* and *CrtISO* transcripts were induced in *PDS*- and *ZDS*-silenced fruits, respectively (Fig. 7). In both cases, the silencing of a desaturase introducing cis double bonds resulted in the induction of the isomerase responsible for their cis- to trans-isomerization. Based on these data, we speculate that two additional regulatory loops, controlling balance between desaturation and isomerization reactions in each functional unit, is acting in tomato fruits (Fig. 8).

Conclusion

To our knowledge, this is the first systematic reverse genetic study of a carotenoid biosynthesis pathway in a higher plant. The data provide several new perspectives on the in vivo functioning of the pathway (Fig. 8): The first dedicated intermediate in the pathway, 15-cis-phytoene, is synthesized largely through the action of PSY1. PSY2 on its own is dispensible, while no firm conclusions can be drawn on a minor redundant role of PSY2/PSY3. Based on the patterns of accumulation of hydroxylated intermediates in fruits silenced at the various biochemical steps, we propose that a parallel desaturation/isomerization pathway exists, involving hydroxylated compounds.

We also propose that two functional units (metabolons), each grouping one desaturase and the downstream isomerase, operate in the tomato fruit pathway, resulting in the accumulation of the earliest intermediate entering the metabolon (15-cis-phytoene and 9,9′-di-cis-ζ-carotene, respectively), when the function of the unit is perturbed. Based on the accumulation of all-trans-ζ-carotene and decrease all-trans-lycopene in ZDS-silenced fruits, and the opposite phenotypes in *CrtISO-L1*- and *CrtISO-L2*-silenced ones, we propose the existence of a competing metabolic branch, initiated by the latter enzymes and proceeding through all-trans-ζ-carotene. We finally propose that three regulatory loops operate on the fruit transcripts. One, described by Kachanovsky et al. (2012), induces the *PSY1* transcript in response to mutations impairing the CrtISO activity. The other two operate within the two proposed functional units and induce the isomerase transcripts (*ZISO* and *CrtISO*, respectively) in response to silencing of the corresponding desaturases

(*PDS* and *ZDS*, respectively). These loops may be sensing the levels of downstream compounds (for instance, prolycopene or a cis-derivative of prolycopene, as proposed by Kachanovsky et al., 2012) or the levels of the enzymes themselves. Further experimentation is needed to clarify this point.

MATERIALS AND METHODS

Plant Material and Growth Conditions

Seeds of the tomato (*Solanum lycopersicum*) F6DR line, transformed with the *Del* and *Ros1* cDNAs under the control of the E8 ripening-specific promoter (Orzaez et al., 2009) as well as the pTRV1, pTRV2/DR, and pTRV2/DR/Gateway T-DNA binary vectors (Orzaez et al., 2009) were kindly provided by Prof. Antonio Granell, Consejo Superior de Investigaciones Científicas. Seeds of tomato cv MM (LA2706), cv Ailsa Craig (LA2838A), and of the isogenic *yellow flesh*^{3532} (LA3532) and *tangerine*^{3183} (LA3183) mutants were obtained from the Tomato Genetics Resource Center (University of California, Davis). Ailsa Craig, *yellow flesh*^{3532}, and *tangerine*^{3183} plants were grown in a greenhouse under a long photoperiod (16-h light/24°C and 8-h dark/20°C). For VIGS experiments, F6DR plants were grown in a growth chamber with controlled photoperiod (16-h light/20°C and 8-h dark/20°C) and irradiance (150 μmol m^{-2} s^{-1}).

Silencing Fragment Selection and Cloning

Silencing fragments were designed using the sequence obtained from the annotation of the tomato genome (ITAG v2.3). Fragments were designed to minimize both the percentage of identity and the length of perfect matches with off-target transcripts (Supplemental Table S2). The sequences of the silencing fragments are shown in Supplemental Figures S3 to S5. The fragments were amplified from cDNA using primers introducing Gateway cloning sites (Supplemental Table S10) and cloned using the Gateway BP Clonase II enzyme mix and Gateway LR Clonase II enzyme according to the manufacturer's protocols.

Fruit Treatment and Harvest

F6DR fruits were labeled when they reached a diameter of about 5 mm. About 4 weeks later, the fruits reached the mature green stage and were agroinfiltrated with an insulin syringe, injecting 1 mL into the fruit through the carpopodium. Drops of infiltration medium appeared on the sepals if the procedure was done correctly. Fruits were inoculated with a 1:1 (v/v) mixture of two *Agrobacterium tumefaciens* C58C1 strains, one containing the pTRV1 vector and the other containing the pTRV2/DR vector with the silencing fragment (or pTRV/DR for the controls). *Agrobacterium* cultures were grown as described earlier, and cell concentration in the infiltration media was adjusted to an outer diameter of 0.05 (Orzaez et al., 2009). Fruits were labeled at the breaker stage of ripening and collected 10 d later. Silenced sectors of the pericarp were separated from nonsilenced (anthocyanin accumulating) ones, frozen in liquid nitrogen, and stored at −80°C for subsequent analyses.

RNA Extraction and Real-Time PCR

RNA was isolated from frozen tissue as described (Lopez-Gomez and Gomez-Lim, 1992). cDNA was synthesized from 0.5 μg of RNA in 20 μL using the RNA PCR kit (Applied Biosystems) according to the manufacturer's instructions with oligo(dT) (16-mer). Quantitative RT-PCR was performed using an ABI Prism 7900HT instrument and a SYBR Green Master Mix kit (Applied Biosystems) using the following protocol: 15 min at 95°C (denaturation) + 1 h at 60°C × 50 cycles. Standard dilution curves were performed for each gene fragment, and all data were normalized for the level of the α-*ACTIN* transcript (similar results were obtained using *ELOGATION FACTOR1*α for normalization). Primers for real-time experiments were designed using the Primer Express v2.0 software and validated with Amplify v3.1 software. Forward and reverse primers were designed on two different exons; at least one of the primers contained at least three mismatches in the 10 nucleotides at the 3′ end, when aligned to nontarget genes in this study. For paralogous genes (*PSY1*, *PSY2*, *PSY3*, *CrtISO*, *CrtISO-L1*, and *CrtISO-L2*), lack of amplification of nontarget genes was verified experimentally using artificial templates. The sequences of the primers are listed in Supplemental Table S11.

Extraction and LC-PDA-MS Analysis of Carotenoids

Five milligrams of lyophilized, homogeneously ground fruit tissue was extracted with 1 mL of methanol:chloroform:50 mM Tris-HCl, pH 7.5 (1:2:1 [v/v]) spiked with 100 mg L^{-1} DL-α-tocopherol acetate (Sigma-Aldrich) as internal standard. After centrifugation, the organic hypophase was removed and the aqueous phase reextracted with the same volume previously used of chloroform spiked with the internal standard. The pooled extracts were dried with a Speed Vac concentrator, and the residue was resuspended in ethyl acetate (100 μL). The extraction was performed in dark conditions keeping samples on ice. Four replicates were performed for each crop. LC-MS analysis was performed using an Accela U-HPLC system monitored with an autosampler and a PDS detector coupled to an LTQ-Orbitrap Discovery mass spectrometer (Thermo Fischer Scientific) operating in positive mode-atmospheric pressure chemical ionization. LC separations were performed using a C30 reverse-phase column (250 × 4.6 mm; YMC Europe). The solvent systems were A, MeOH; B, MeOH/water (4:1 [v/v]) and 0.2% ammonium acetate; and C, *tert*-butyl-methyl ether. The gradient elution was as follows: 0 to 6 min 95% A, 5% B, and 0% C; 1 min 80% A, 5% B, and 15% C; 5 min 80% A, 5% B, and 15% C; 20 min 30% A, 5% B, and 65% C; 22 min 30% A, 5% B, and 65%C; 18 min 95% A, 5% B, and 0% C. The flow rate was 1 mL min^{-1}. Chemicals and solvents were LC-MS grade quality from Sigma-Aldrich (Chromasolv). The atmospheric pressure chemical ionization-MS ionization parameters were as follows: from 0 to 20 min, 20 units of nitrogen (sheath gas) and five units of auxiliary gas were used, respectively; the vaporizer temperature was 225°C, the capillary temperature was 175°C, the discharge current was 5.0 μA, and the capillary voltage and tube lens settings were 49 V and 129 V, respectively. From 20 to 33 min, 20 and 10 units of nitrogen sheath and auxiliary gas, respectively, were used; vaporizer and capillary temperatures were 250°C and 370°C, respectively, discharge current was 5.0 μA, capillary voltage was 17 V, and tube lens settings was 90 V. From 34 to 54 min, sheath and auxiliary gas were 20 and 5 units, respectively; vaporizer temperature was 350°C, capillary temperature was 250°C, discharge current was 5.0 μA, and capillary voltage and tube lens settings were 17 and 10 V, respectively. Carotenoids were identified by their order of elution and online absorption spectra (Lee and Chen, 2001; Rodriguez-Amaya, 2001; Isaacson et al., 2004; Breitenbach and Sandmann, 2005; Fraser et al., 2007; Li et al., 2007; Chen et al., 2010; Yu et al., 2011), comigration with authentic standards (all-trans-lycopene, all-trans-α-carotene, all-trans-δ-carotene, all-trans-β-carotene, lutein, all-trans-violaxanthin, and all-trans-neoxanthin), and on the basis of the m z^{-1} accurate masses obtained from the Pubchem database (http://pubchem.ncbi.nlm.nih.gov/) for native compounds or from the Metabolomics Fiehn Lab Mass Spectrometry Adduct Calculator (http://fiehnlab.ucdavis.edu/staff/kind/Metabolomics/MS-Adduct-Calculator/) for adducts. Carotenoid peaks were integrated at their individual λmax and DL-α-tocopherol acetate at 285 nm (Fraser et al., 2000). For normalization and quantification, all peaks were normalized relative to the internal standard (DL-α-tocopherol acetate) to correct for extraction and injection variability. An external calibration curve of DL-α-tocopherol acetate, run separately, was used to calculate absolute amounts. All carotenoid peaks underwent a second normalization to correct for their individual molar extinction coefficients (Rodriguez-Amaya, 2001). Statistical analysis (one-way ANOVA plus Tukey's pairwise comparison) was performed using the PAST software (Hammer et al., 2001).

Supplemental Data

The following materials are available in the online version of this article.

Supplemental Figure S1. Schematic representation of the pTRV1 and pTRV2 constructs.

Supplemental Figure S2. Chromosomal position of the analyzed genes.

Supplemental Figure S3. Silencing fragment selection for the *PSY* transcripts.

Supplemental Figure S4. Silencing fragment selection for the *CrtISO* and *CrtISO-L* transcripts.

Supplemental Figure S5. Silencing fragment selection for the *PDS*, *ZDS*, and *ZISO* transcripts.

Supplemental Figure S6. Silencing efficiency of the different constructs.

Supplemental Figure S7. Phylogenetic analysis of the PSY proteins.

Supplemental Figure S8. Phylogenetic analysis of the CrtISO proteins.

Supplemental Figure S9. Online PDA spectra of compounds indicated in Supplemental Table S3.

Supplemental Figure S10. *PSY1* and *PDS* expression levels in *r* and *t* mutant ripe fruits.

Supplemental Table S1. Normalized expression (FPKM) of candidate lycopene biosynthesis genes in different tissues of tomato, analyzed by Illumina RNA-Seq.

Supplemental Table S2. Off-target homology of the silencing fragments.

Supplemental Table S3. Identification of carotenoids from ripe tomato fruits.

Supplemental Table S4. Carotenoid composition of F6DR, TRV/DR-silenced sectors, Moneymaker (MM), and Ailsa Craig (AC) fruits ($\mu g\ g^{-1}$ dry weight).

Supplemental Table S5. Carotenoid composition of fruit sectors silenced with gene-specific constructs, compared with those silenced with vector alone ($\mu g\ g^{-1}$ dry weight).

Supplemental Table S6. Fruit carotenoid composition of Ailsa Craig (LA2838A) and of its isogenic *yellow flesh* (LA3532) and *tangerine*^{3183} (LA3183) mutants ($\mu g\ g^{-1}$ dry weight).

Supplemental Table S7. Carotenoid composition of silenced sectors from light- and dark-grown fruits ($\mu g\ g^{-1}$ dry weight).

Supplemental Table S8. Isomeric composition of silenced fruit sectors ($\mu g\ g^{-1}$ dry weight).

Supplemental Table S9. Isomeric composition of silenced sectors from light- and dark-grown fruits ($\mu g\ g^{-1}$ dry weight).

Supplemental Table S10. attB PCR primers used for silencing fragment amplification.

Supplemental Table S11. Primers used for real-time PCR.

ACKNOWLEDGMENTS

We thank Drs. Antonio Granell and Diego Orzaez (Consejo Superior de Investigaciones Científicas, Valencia) for the pTRV1, pTRV2/DR, and pTRV2/DR/Gateway silencing vectors and F6DR tomato seeds. We also thank Drs. Gianfranco Diretto and Roberto Ciccoli for helpful discussions and suggestions on LC-MS methods, and Dr. Marco Pietrella for helping with RNA-Seq data management.

Received July 11, 2013; accepted September 4, 2013; published September 6, 2013.

LITERATURE CITED

Alba R, Cordonnier-Pratt MM, Pratt LH (2000) Fruit-localized phytochromes regulate lycopene accumulation independently of ethylene production in tomato. Plant Physiol **123:** 363–370

Alder A, Jamil M, Marzorati M, Bruno M, Vermathen M, Bigler P, Ghisla S, Bouwmeester H, Beyer P, Al-Babili S (2012) The path from β-carotene to carlactone, a strigolactone-like plant hormone. Science **335:** 1348–1351

Bartley GE, Scolnik PA, Beyer P (1999) Two *Arabidopsis thaliana* carotene desaturases, phytoene desaturase and zeta-carotene desaturase, expressed in *Escherichia coli*, catalyze a poly-cis pathway to yield prolycopene. Eur J Biochem **259:** 396–403

Baulcombe DC (1999) Fast forward genetics based on virus-induced gene silencing. Curr Opin Plant Biol **2:** 109–113

Bonk M, Hoffmann B, Von Lintig J, Schledz M, Al-Babili S, Hobeika E, Kleinig H, Beyer P (1997) Chloroplast import of four carotenoid biosynthetic enzymes in vitro reveals differential fates prior to membrane binding and oligomeric assembly. Eur J Biochem **247:** 942–950

Breitenbach J, Sandmann G (2005) zeta-Carotene cis isomers as products and substrates in the plant poly-cis carotenoid biosynthetic pathway to lycopene. Planta **220:** 785–793

Busch M, Seuter A, Hain R (2002) Functional analysis of the early steps of carotenoid biosynthesis in tobacco. Plant Physiol **128:** 439–453

Candau R, Bejarano ER, Cerdá-Olmedo E (1991) In vivo channeling of substrates in an enzyme aggregate for beta-carotene biosynthesis. Proc Natl Acad Sci USA **88:** 4936–4940

Chen Y, Li F, Wurtzel ET (2010) Isolation and characterization of the *Z-ISO* gene encoding a missing component of carotenoid biosynthesis in plants. Plant Physiol **153:** 66–79

Clough JM, Pattenden G (1983) Stereochemical assignment of prolycopene and other poly-*Z*-isomeric carotenoids in fruits of the tangerine tomato *Lycopersicon esculentum* var. "Tangella". J Chem Soc Perkin 1 **1:** 3011–3018

Corona V, Aracri B, Kosturkova G, Bartley GE, Pitto L, Giorgetti L, Scolnik PA, Giuliano G (1996) Regulation of a carotenoid biosynthesis gene promoter during plant development. Plant J **9:** 505–512

Curl AL (1961) The xanthophylls of tomatoes. J Food Sci **26:** 106–111

Dong H, Deng Y, Mu J, Lu Q, Wang Y, Xu Y, Chu C, Chong K, Lu C, Zuo J (2007) The *Arabidopsis* Spontaneous Cell Death1 gene, encoding a zeta-carotene desaturase essential for carotenoid biosynthesis, is involved in chloroplast development, photoprotection and retrograde signalling. Cell Res **17:** 458–470

Fraser PD, Enfissi EM, Halket JM, Truesdale MR, Yu D, Gerrish C, Bramley PM (2007) Manipulation of phytoene levels in tomato fruit: effects on isoprenoids, plastids, and intermediary metabolism. Plant Cell **19:** 3194–3211

Fraser PD, Pinto ME, Holloway DE, Bramley PM (2000) Technical advance: application of high-performance liquid chromatography with photodiode array detection to the metabolic profiling of plant isoprenoids. Plant J **24:** 551–558

Fray RG, Grierson D (1993) Identification and genetic analysis of normal and mutant phytoene synthase genes of tomato by sequencing, complementation and co-suppression. Plant Mol Biol **22:** 589–602

Fray RG, Wallace A, Fraser PD, Valero D, Hedden P, Bramley PM, Grierson D (1995) Constitutive expression of a fruit phytoene synthase gene in transgenic tomatoes causes dwarfism by redirecting metabolites from the gibberellin pathway. Plant J **8:** 693–701

Fu DQ, Zhu BZ, Zhu HL, Jiang WB, Luo YB (2005) Virus-induced gene silencing in tomato fruit. Plant J **43:** 299–308

Giliberto L, Perrotta G, Pallara P, Weller JL, Fraser PD, Bramley PM, Fiore A, Tavazza M, Giuliano G (2005) Manipulation of the blue light photoreceptor cryptochrome 2 in tomato affects vegetative development, flowering time, and fruit antioxidant content. Plant Physiol **137:** 199–208

Giuliano G, Bartley GE, Scolnik PA (1993) Regulation of carotenoid biosynthesis during tomato development. Plant Cell **5:** 379–387

Giuliano G, Giliberto L, Rosati C (2002) Carotenoid isomerase: a tale of light and isomers. Trends Plant Sci **7:** 427–429

Giuliano G, Pollock D, Stapp H, Scolnik PA (1988) A genetic-physical map of the *Rhodobacter capsulatus* carotenoid biosynthesis gene cluster. Mol Gen Genet **213:** 78–83

Hable WE, Oishi KK, Schumaker KS (1998) Viviparous-5 encodes phytoene desaturase, an enzyme essential for abscisic acid (ABA) accumulation and seed development in maize. Mol Gen Genet **257:** 167–176

Hammer Ø, Harper DAT, Ryan PD (2001) PAST: paleontological statistics software package for education and data analysis. Palaeontol Electronica **4:** 1–9

Isaacson T, Ohad I, Beyer P, Hirschberg J (2004) Analysis in vitro of the enzyme CRTISO establishes a poly-cis-carotenoid biosynthesis pathway in plants. Plant Physiol **136:** 4246–4255

Isaacson T, Ronen G, Zamir D, Hirschberg J (2002) Cloning of tangerine from tomato reveals a carotenoid isomerase essential for the production of beta-carotene and xanthophylls in plants. Plant Cell **14:** 333–342

Kachanovsky DE, Filler S, Isaacson T, Hirschberg J (2012) Epistasis in tomato color mutations involves regulation of phytoene synthase 1 expression by cis-carotenoids. Proc Natl Acad Sci USA **109:** 19021–19026

Lee MT, Chen BH (2001) Separation of lycopene and its cis isomers by liquid chromatography. Chromatographia **54:** 613–617

Lewinsohn E, Sitrit Y, Bar E, Azulay Y, Meir A, Zamir D, Tadmor Y (2005) Carotenoid pigmentation affects the volatile composition of tomato and watermelon fruits, as revealed by comparative genetic analyses. J Agric Food Chem **53:** 3142–3148

Li F, Murillo C, Wurtzel ET (2007) Maize *Y9* encodes a product essential for 15-cis-zeta-carotene isomerization. Plant Physiol **144:** 1181–1189

Li F, Vallabhaneni R, Wurtzel ET (2008) *PSY3*, a new member of the phytoene synthase gene family conserved in the Poaceae and regulator of abiotic stress-induced root carotenogenesis. Plant Physiol **146:** 1333–1345

Liang D, Finnegan EJ, Dennis ES, Waterhouse PM, Wang M-B (2011) Mobile silencing in plants: what is the signal and what defines the target. Front Biol **6:** 140–146

Liu Y, Schiff M, Dinesh-Kumar SP (2002) Virus-induced gene silencing in tomato. Plant J **31:** 777–786

Lopez AB, Yang Y, Thannhauser TW, Li L (2008) Phytoene desaturase is present in a large protein complex in the plastid membrane. Physiol Plant **133:** 190–198

Lopez-Gomez R, Gomez-Lim MA (1992) A method for extracting intact RNA from fruits rich in polysaccharides using ripe mango mesocarp. HortScience **27:** 440–442

Moore MJ, Soltis PS, Bell CD, Burleigh JG, Soltis DE (2010) Phylogenetic analysis of 83 plastid genes further resolves the early diversification of eudicots. Proc Natl Acad Sci USA **107:** 4623–4628

Orzaez D, Medina A, Torre S, Fernández-Moreno JP, Rambla JL, Fernández-Del-Carmen A, Butelli E, Martin C, Granell A (2009) A visual reporter system for virus-induced gene silencing in tomato fruit based on anthocyanin accumulation. Plant Physiol **150:** 1122–1134

Park H, Kreunen SS, Cuttriss AJ, DellaPenna D, Pogson BJ (2002) Identification of the carotenoid isomerase provides insight into carotenoid biosynthesis, prolamellar body formation, and photomorphogenesis. Plant Cell **14:** 321–332

Qin G, Gu H, Ma L, Peng Y, Deng XW, Chen Z, Qu LJ (2007) Disruption of phytoene desaturase gene results in albino and dwarf phenotypes in *Arabidopsis* by impairing chlorophyll, carotenoid, and gibberellin biosynthesis. Cell Res **17:** 471–482

Quinlan RF, Shumskaya M, Bradbury LM, Beltrán J, Ma C, Kennelly EJ, Wurtzel ET (2012) Synergistic interactions between carotene ring hydroxylases drive lutein formation in plant carotenoid biosynthesis. Plant Physiol **160:** 204–214

Rao AV, Agarwal S (2000) Role of antioxidant lycopene in cancer and heart disease. J Am Coll Nutr **19:** 563–569

Rodriguez-Amaya DB (2001) A Guide to Carotenoid Analysis in Foods. ILSI Press, Washington, DC

Romero I, Tikunov Y, Bovy A (2011) Virus-induced gene silencing in detached tomatoes and biochemical effects of phytoene desaturase gene silencing. J Plant Physiol **168:** 1129–1135

Sato S, Tabata S, Hirakawa H, Asamizu E, Shirasawa K, Isobe S, Kaneko T, Nakamura Y, Shibata D, Aoki K, et al, Tomato Genome Consortium (2012) The tomato genome sequence provides insights into fleshy fruit evolution. Nature **485:** 635–641

Sweetlove LJ, Fernie AR (2013) The spatial organization of metabolism within the plant cell. Annu Rev Plant Biol **64:** 723–746

Welsch R, Wüst F, Bär C, Al-Babili S, Beyer P (2008) A third phytoene synthase is devoted to abiotic stress-induced abscisic acid formation in rice and defines functional diversification of phytoene synthase genes. Plant Physiol **147:** 367–380

Xu P, Zhang Y, Kang L, Roossinck MJ, Mysore KS (2006) Computational estimation and experimental verification of off-target silencing during posttranscriptional gene silencing in plants. Plant Physiol **142:** 429–440

Yu Q, Ghisla S, Hirschberg J, Mann V, Beyer P (2011) Plant carotene cis-trans isomerase CRTISO: a new member of the FAD(RED)-dependent flavoproteins catalyzing non-redox reactions. J Biol Chem **286:** 8666–8676